

Rare K decays in a model of quark and lepton masses

P. Q. Hung*, Andrea Soddu*

Dept. of Physics, University of Virginia,

382 McCormick Road, P. O. Box 400714, Charlottesville, Virginia 22904-4714

(May 20, 2019)

Abstract

An extension of a model of neutrino masses to the quark sector provides an interesting link between these two sectors. A parameter which is important to describe neutrino oscillations and masses is found to be a crucial one appearing in various “penguin” operators, in particular the so-called Z penguin. This parameter is severely constrained by the rare decay process $K_L \rightarrow \mu^+ \mu^-$. This in turn has interesting implications on the decay rates of other rare processes such as $K_L \rightarrow \mu e$, etc..., as well as on the masses of the neutrinos and the masses of the vector-like quarks and leptons which appear in our model.

12.15.Ff, 12.60.Cn, 13.20.Eb, 14.60.Pq, 14.60.St, 14.70.Pw

I. INTRODUCTION

In the last few years, we have witnessed a flurry of far-reaching experimental results, among which are the neutrino oscillation data [1], data on direct CP-violation such as ϵ'/ϵ [2] and upper bounds on Flavour-Changing-Neutral-Current (FCNC) rare decays of the kaons. On the one hand, the neutrino oscillation data clearly points to possible physics beyond the Standard Model (SM). On the other hand, it is still not clear if the new results on ϵ'/ϵ , which differ roughly by a factor of two from present calculations within the SM, imply any new physics since the aforementioned calculations are still plagued with non-perturbative uncertainties. For the kaon's FCNC rare decays, the experimental situation is still far from giving evidences of physics beyond the SM or to confirm the SM itself. Nevertheless, whatever new physics, which might be responsible for giving rise to neutrino masses, could, in principle, affect the quark sector, and hence, also quantities such as ϵ'/ϵ or the branching ratios of the kaon's FCNC rare decays. If this is the case, results from the quark sector could then be used to put constraints on the lepton sector itself since it is possible that both sectors have a common set of parameters, a desirable feature of any model which purports to deal with issues of fermion masses. The aim of this paper is to explore this possible connection between the two sectors.

The subject of neutrino masses has been invigorated in the last few years due to new results on neutrino oscillations which suggested the possibility of a non-vanishing mass for the neutrinos. Models have been (and are still being) built to try to describe these oscillations. In a large number of cases, efforts were mainly concentrated on the type of neutrino mass matrices which could “explain” the oscillation data, with very little attempt made in trying to connect that kind of physics to the hadronic sector. However, it is perfectly reasonable to expect that the two sectors are somehow deeply connected, and that a constraint from one sector can give rise to constraints on the other sector. This particular connection will be the subject of the present manuscript. This paper is an extension to the quark sector of a model of neutrino mass presented in Ref. [3]. In consequence, we shall show that there is

a set of parameters which appear in both sectors, and that the constraints obtained in the quark sector have interesting implications on the neutrino sector. In particular, we shall use recent results from limits on various rare decays to constrain a common parameter which appears in both sectors. (As we will show, because this common parameter is real, there will be no new contributions from our model to ϵ'/ϵ .)

The plan of this paper is as follows. First, we present our model for the quark sector based on a previous model for the neutrino sector [3]. We then proceed to enumerate and compute various FCNC operators which arise in this model. These operators are important in the analysis of various rare decays. Finally, we will use these FCNC operators in the computation of their contributions to the aforementioned quantities, and set constraints on the parameters of the model. Using these constraints, we look at the question of how they would affect the neutrino sector. We will also show at the end of the paper that there are some interesting correlations between the value of the branching ratio for $K_L \rightarrow \mu^+\mu^-$ and the mass of the weak-singlet quarks and charged leptons which appear in our model. When these particles are “light” enough to be produced at future accelerators, the branching ratio for $K_L \rightarrow \mu^+\mu^-$ is too small, of order 10^{-22} , to be detected, while for a branching ratio which could conceivably be measured in a not-too-distant future, e.g. of order 10^{-14} , the masses of these singlet quarks and leptons will be too large, a few hundreds of TeVs or more, to be produced by earthbound laboratories.

II. EFFECTIVE VERTICES FOR FCNC PROCESSES IN THE MODEL OF REF. [3]

The model used in Ref. [3] to describe the lepton sector is summarized in Appendix A. (A quick look at that appendix will help with the notations and particle content.) In this section, we will simply write down the part of the Lagrangian for the quark sector which is relevant to the construction of various FCNC operators. First of all, the common link between the quark and lepton sectors is in the scalar sector. These are the SM Higgs field

ϕ and the Family symmetry Higgs field Ω^α . As we shall see below, it is these scalars which “transmit information” from the quark to the lepton sector and vice versa. In particular, as can be seen from Appendix A, Ω^α provides the common set of parameters which appears in the two sectors. The generalization from the lepton sector to the quark sector necessitates the introduction of a new set of vector-like quarks, F^i , \mathcal{M}_1^i , and \mathcal{M}_2^i , where i is a color index, in perfect analogy with the leptonic vector-like fermions, F , \mathcal{M}_1 , and \mathcal{M}_2 . As we shall see below, these vector-like quarks can have masses as low as a couple of hundred GeV’s, making them very attractive for potential discoveries at the LHC. We shall come back to this interesting issue in the last section of the manuscript.

The particle content and quantum numbers of the model are listed in Table 1. Notice that, among the scalars listed in that table, there is one which does not have the appropriate quantum numbers to be able to couple directly to the quarks: ρ^α . The gauge structure of the model (for both quarks and leptons) is given by:

$$SU(3)_c \otimes SU(2)_L \otimes U(1)_Y \otimes SO(4) \otimes SU(2)_{\nu_R}, \quad (1)$$

where $SU(2)_{\nu_R}$ applies only to the right-handed neutrinos, and $SO(4)$ is the family symmetry. The form of the quark Yukawa Lagrangian is similar to the one from the lepton sector (Appendix A), with the introduction of the following new parameters:

$$g_u, g_d, G_1, G_2, G_3, G_{\mathcal{M}_1}, G_{\mathcal{M}_2}, M_F, M_{\mathcal{M}_1}, M_{\mathcal{M}_2}. \quad (2)$$

The quark Yukawa Lagrangian takes the form

$$\begin{aligned} \mathcal{L}_{quark}^Y = & g_d \bar{q}_L^\alpha \phi d_{\alpha R} + g_u \bar{q}_L^\alpha \tilde{\phi} u_{\alpha R} + \\ & G_1 \bar{q}_L^\alpha \Omega_\alpha F_R + G_{\mathcal{M}_1} \bar{F}_L \phi \mathcal{M}_{1R} + G_{\mathcal{M}_2} \bar{F}_L \tilde{\phi} \mathcal{M}_{2R} + \\ & G_2 \bar{\mathcal{M}}_{1L} \Omega_\alpha d_R^\alpha + G_3 \bar{\mathcal{M}}_{2L} \Omega_\alpha u_R^\alpha + \\ & M_F \bar{F}_L F_R + M_{\mathcal{M}_1} \bar{\mathcal{M}}_{1L} \mathcal{M}_{1R} + \\ & M_{\mathcal{M}_2} \bar{\mathcal{M}}_{2L} \mathcal{M}_{2R} + h.c., \end{aligned} \quad (3)$$

with the important difference with respect to the lepton sector in that there is no coupling between the quarks and the scalar ρ^α before symmetry breaking. After symmetry breaking,

the mass eigenstates are linear combinations of Ω and ρ , and vice versa, as shown below and in Appendix A.

The way the FCNC processes take place in the quark sector is identical to the way they operate in the lepton sector i.e. via loop diagrams. In the SM, as it is well known, the flavour diagonal structure of the basic vertices involving γ , Z and g forbids the appearance of FCNC processes at the tree level. However the FCNC processes can happen at one loop or higher order level, mediated by a combination of flavour changing charged currents coupled to the W 's. The fact that these processes take place only as loop effects makes them particularly useful for testing the quantum structure of the theory and in search for physics beyond the SM. In our model, beside the ways in which FCNC processes can happen in the SM, it can also happen because of the couplings of quarks of different flavour to the same vector-like fermion F and to the NG bosons $\tilde{\Omega}_i$ and the pseudo NG bosons $Re\tilde{\rho}_i$. This is made possible by the mixings among the NG bosons $\tilde{\Omega}_i$ and the pseudo NG bosons $Re\tilde{\rho}_j$ with different family indices i and j . We denote the relevant scalar mass eigenstates by $\tilde{\Omega}_i$ and $Re\tilde{\rho}_i$, in terms of which we can express the states entering the Yukawa Lagrangian by

$$\Omega_i = \cos \beta \tilde{\Omega}_i - \sin \beta Re\tilde{\rho}_i, \quad (4)$$

$$Re\rho_i = \sin \beta \tilde{\Omega}_i + \cos \beta Re\tilde{\rho}_i. \quad (5)$$

The states $\tilde{\Omega}_i$ are the NG bosons which are absorbed by the corresponding family gauge bosons. When the NG bosons get mixed, there will be mass mixings among the corresponding family gauge bosons. If we denote by A_Ω the orthogonal matrix which diagonalizes the family gauge bosons mass matrix (Ref. [3]), we can express the states $\tilde{\Omega}'_i$, corresponding to the longitudinal components of the gauge boson mass eigenstates, in terms of the mass eigenstates $\tilde{\Omega}_i$

$$\tilde{\Omega}_i = A_{\Omega,ij}^T \tilde{\Omega}'_j, \quad (6)$$

with A_Ω given by

$$A_\Omega = \begin{pmatrix} \frac{1}{\sqrt{2}} & \frac{1}{\sqrt{2}} & 0 \\ -\frac{1}{\sqrt{2}} & \frac{1}{\sqrt{2}} & 0 \\ 0 & 0 & 1 \end{pmatrix}. \quad (7)$$

This mechanism, introduced to describe neutrino mass splitting in the neutral lepton sector, gives the following terms in the Yukawa Lagrangian:

$$\begin{aligned} G_1 \bar{q}_L^i \Omega_i F_R &= \cos \beta G_1 \bar{q}_L^i \tilde{\Omega}_i F_R - \sin \beta G_1 \bar{q}_L^i \text{Re} \tilde{\rho}_i F_R \\ &= \cos \beta G_1 \bar{q}_L^i A_{\Omega,ij}^T \tilde{\Omega}'_j F_R - \sin \beta G_1 \bar{q}_L^i A_{\Omega,ij}^T \text{Re} \tilde{\rho}'_j F_R, \end{aligned} \quad (8)$$

$$\begin{aligned} G_2 \bar{\mathcal{M}}_{1L} \Omega_i d_R^i &= \cos \beta G_2 \bar{\mathcal{M}}_{1L} \tilde{\Omega}_i d_R^i - \sin \beta G_2 \bar{\mathcal{M}}_{1L} \text{Re} \tilde{\rho}_i d_R^i \\ &= \cos \beta G_2 \bar{\mathcal{M}}_{1L} A_{\Omega,ij}^T \Omega'_j d_R^i - \sin \beta G_2 \bar{\mathcal{M}}_{1L} A_{\Omega,ij}^T \text{Re} \tilde{\rho}'_j d_R^i, \end{aligned} \quad (9)$$

where we assume that the same A_Ω diagonalizes also the mass matrix of the pseudo NG $\text{Re} \tilde{\rho}_i$ (Ref. [3]). It is important to notice here that H_4 and h_4 , whose mass eigenstates are given by \tilde{H}_4 and \tilde{h}_4 , see Eq. 10, are not coupled to the quarks of the first three families. This implies that they will not propagate in the loops of the diagrams describing processes with external quarks of the first three generations. In this paper we will look only at processes involving the quarks of the first three families and so we will not care about the presence in our model of H_4 and h_4 , where

$$\begin{aligned} \tilde{H}_4 &= \cos \alpha H_4 + \sin \alpha h_4, \\ \tilde{h}_4 &= -\sin \alpha H_4 + \cos \alpha h_4. \end{aligned} \quad (10)$$

In the following we will present the expressions of the effective vertices for FCNC processes mediated by Z , γ , and g . There is no extra effective vertex with the SM Higgs in our model because the vector-like fermions do not couple to the SM Higgs field. We will also compare these expressions with the corresponding ones from the SM.

For all the effective vertices, the expressions will be given in terms of the linear combination

$$\mathcal{M} = \mathcal{M}_\Omega \cos^2 \beta + \mathcal{M}_\rho \sin^2 \beta, \quad (11)$$

where \mathcal{M}_Ω and \mathcal{M}_ρ are the contributions to the effective vertices when the particles propagating in the loops are respectively the NG bosons $\tilde{\Omega}'_i$ and the pseudo NG bosons $Re\tilde{\rho}'_i$. From the lepton sector we have estimated $\tan \beta$ to be

$$\tan \beta \equiv \frac{V'}{V} \approx g_F^2 \frac{M_F^L M_{\mathcal{M}_2}^L}{M_G^2}, \quad (12)$$

with g_F being the $SO(4)$ gauge coupling. V' and V are the vacuum expectation values (VEV) of ρ and Ω respectively, M_F^L and $M_{\mathcal{M}_2}^L$ the masses of the vector-like fermions introduced in the lepton sector, and M_G the central value for the masses of the family gauge bosons. Taking $g_F \sim O(1)$, and, for the masses, the values required in the lepton sector to have a proper value for the neutrino of the 4th generation, $\tan \beta$ turns out to be much smaller than unity. This makes the contribution to \mathcal{M} due to the pseudo NG bosons negligible, being suppressed by the factor $\sin^2 \beta$. In the following we will give only the expressions for the contributions due to the NG bosons $\tilde{\Omega}'_i$. All the expressions that will be given for the effective vertices will have to be multiplied by the factor $\cos^2 \beta$. We will focus on the expressions for the effective vertices in the transition $s \rightarrow d$.

III. THE Z EFFECTIVE VERTEX

To calculate the Z effective vertex we have to sum up all the contributions coming from the different vector-like fermions propagating in the loop diagrams. We will present separately the expressions for the amplitude due respectively to the F_d and \mathcal{M}_1 vector-like fermions. We remark here that F_d is the down component of a doublet of $SU(2)_L$ while \mathcal{M}_1 is a singlet of $SU(2)_L$ (see Table 1). Because the dominant terms of the amplitudes are proportional to T_{3L} of the vector-like fermions, the contribution due to F_d is singled out. The contribution from \mathcal{M}_1 will be suppressed by the factor $1/M_G^2$ with M_G being the scale of breaking of the family symmetry. The amplitude due to F_d is as follows

$$\mathcal{M}_Z^{F,\mu} = \frac{-ig}{16\pi^2 \cos(\theta_W)} g_F^2 \sum_{j=1}^3 A_{\Omega,2j}^T A_{\Omega,j} 2(g_- - g_+) \left[\frac{1}{2} \ln \frac{M_{\Omega_j}^2}{M_F^2} + \frac{1}{2} \frac{M_F^2}{M_F^2 - M_{\Omega_j}^2} + \frac{1}{2} \left(\frac{M_F^2}{M_F^2 - M_{\Omega_j}^2} \right)^2 \ln \frac{M_{\Omega_j}^2}{M_F^2} - \frac{M_F^2}{M_F^2 - M_{\Omega_j}^2} \ln \frac{M_{\Omega_j}^2}{M_F^2} \right] \bar{s} \gamma^\mu (1 - \gamma^5) d, \quad (13)$$

where

$$g_- - g_+ = -g_A = -T_{3L} = \frac{1}{2}, \quad (14)$$

It is important to notice here that with M_{Ω_j} we have indicated the poles in the propagators of the longitudinal components of the gauge boson mass eigenstates $\tilde{\Omega}'_i$.

Using for M_{Ω_j} the eigenvalues of the family gauge boson mass matrix in the simplistic form introduced for the lepton sector

$$\mathcal{M}_G^2 = M_G^2 \begin{pmatrix} 1 & b & 0 \\ b & 1 & 0 \\ 0 & 0 & 1 \end{pmatrix}, \quad (15)$$

given by

$$\begin{aligned} M_{\Omega_1}^2 &= M_G^2 (1 + b), \\ M_{\Omega_2}^2 &= M_G^2 (1 - b), \\ M_{\Omega_3}^2 &= M_G^2, \end{aligned} \quad (16)$$

where b is a small parameter less than unity, and the orthogonal matrix A_Ω is given in Eq. 7, we obtain the following final expression for $\mathcal{M}_Z^{F,\mu}$

$$\mathcal{M}_Z^{F,\mu} = \frac{-ig}{16\pi^2 \cos(\theta_W)} g_F^2 C_0(x_F, b) \bar{s} \gamma^\mu (1 - \gamma^5) d, \quad (17)$$

with

$$\begin{aligned} C_0(x_F, b) &= \frac{1}{4(1+b-x_F)^2(-1+b+x_F)^2} \left[-(-1+b)^2(1+b-x_F)^2 \ln(1-b) \right. \\ &\quad \left. + (1+b)^2(-1+b+x_F)^2 \ln(1+b) \right. \\ &\quad \left. - 2bx_F(b^2 - (-1+x_F)^2 + 2(-1+b^2+x_F) \ln(x_F)) \right], \end{aligned} \quad (18)$$

where x_F is defined as

$$x_F = \frac{M_F^2}{M_G^2}. \quad (19)$$

Making the Taylor expansion of $C_0(x_F, b)$ in the parameter b we found that the first non zero contribution comes from the linear term in b . So we can rewrite $C_0(x_F, b)$ as

$$C_0(x_F, b) = b C_0(x_F) + \mathcal{O}(b^2), \quad (20)$$

with $C_0(x_F)$ given by

$$C_0(x_F) = \frac{1}{2} \left[\frac{1 + x_F}{(1 - x_F)^2} + \frac{2x_F}{(1 - x_F)^3} \ln x_F \right]. \quad (21)$$

$\mathcal{M}_Z^{F,\mu}$ now takes the simple form

$$\mathcal{M}_Z^{F,\mu} = \frac{-ig}{16\pi^2 \cos(\theta_W)} g_F^2 b C_0(x_F) \bar{s} \gamma^\mu (1 - \gamma^5) d + \mathcal{O}(b^2), \quad (22)$$

which shows, in the first approximation, an explicit linear dependence on the parameter b . In Appendix B, it will be shown in a simple example the mechanism that produces the b dependence of the amplitude for FCNC processes and it will be compared with the GIM mechanism.

The contribution to the Z effective vertex due to \mathcal{M}_1 takes the form

$$\mathcal{M}_Z^{\mathcal{M}_1,\mu} = \frac{ig \sin^2(\theta_W)}{16\pi^2 \cos(\theta_W)} \frac{g_F^2}{4M_{\mathcal{M}_1}^2} D_0(x_M, b) \bar{s}(q^2 \gamma^\mu - q^\mu \not{q})(1 + \gamma^5) d, \quad (23)$$

where q is the momentum transfer and with

$$D_0(x_M, b) = \left[\frac{b \left(-5b^4 + (-1 + x_M)^2 (5 + x_M) (-1 + 7x_M) \right)}{(1 + b - x_M)^3 (-1 + b + x_M)^3} + \frac{2b^3 (5 + x_M) (-22 + 23x_M)}{(1 + b - x_M)^3 (-1 + b + x_M)^3} - \frac{3(-1 + b)^2 (-1 + b + 3x_M) \ln\left(\frac{x_M}{1-b}\right)}{(-1 + b + x_M)^4} - \frac{3(1 + b)^2 (1 + b - 3x_M) \ln\left(\frac{x_M}{1+b}\right)}{(1 + b - x_M)^4} \right] \frac{x_M}{27}, \quad (24)$$

where x_M is defined as

$$x_M = \frac{M_{\mathcal{M}_1}^2}{M_G^2}. \quad (25)$$

It is important to notice here that the structure of the operator in $\mathcal{M}_Z^{\mathcal{M}_1, \mu}$ is similar in character to that for the photon. In fact, $q_\mu \mathcal{M}_Z^{\mathcal{M}_1, \mu} = 0$. This happens because \mathcal{M}_1 is a singlet of $SU(2)$ and so the current of \mathcal{M}_1 that couples to Z has the vectorial nature characteristic of the currents interacting with the photon. Making a Taylor expansion of the function $D_0(x_M, b)$ in the parameter b we found also that in this case the first non vanishing term in the expansion is that one linear in b . So we can rewrite $D_0(x_M, b)$ as

$$D_0(x_M, b) = b D_0(x_M) + \mathcal{O}(b^2), \quad (26)$$

with $D_0(x_M)$ given by

$$D_0(x_M) = \frac{x_M}{27} \left[\frac{11 + 6 \ln x_M - 18 x_M \ln x_M - 63 x_M + 45 x_M^2 + 7 x_M^3 - 36 x_M^2 \ln x_M}{(1 - x_M)^5} \right]. \quad (27)$$

Now $\mathcal{M}_Z^{\mathcal{M}_1, \mu}$ takes the simple form

$$\mathcal{M}_Z^{\mathcal{M}_1, \mu} = \frac{ig \sin^2(\theta_W)}{16\pi^2 \cos(\theta_W)} \frac{g_F^2}{4M_{M_1}^2} b D_0(x_M) \bar{s}(q^2 \gamma^\mu - q^\mu \not{q})(1 + \gamma^5) d + \mathcal{O}(b^2). \quad (28)$$

For comparison we show the explicit expression of the corresponding contribution from the SM, as given in Ref. [4].

$$\mathcal{M}_Z^{SM, \mu} = \frac{ig}{16\pi^2 \cos(\theta_W)} g^2 V_{ts}^* V_{td} C_0^{SM}(x_t) \bar{s} \gamma^\mu (1 - \gamma^5) d, \quad (29)$$

where

$$C_0^{SM}(x_t) = \frac{x_t}{8} \left[\frac{x_t - 6}{x_t - 1} + \frac{3x_t + 2}{(x_t - 1)^2} \ln x_t \right], \quad (30)$$

with x_t defined as

$$x_t = \frac{m_t^2}{M_W^2}, \quad (31)$$

and g is the $SU(2)_L$ gauge coupling.

IV. THE γ EFFECTIVE VERTEX

The effective vertex of γ comes also from the contributions due the F_d and \mathcal{M}_1 vector-like fermions. What is remarkable is that these two contributions will contain the *same function* D_0 (Eq. 24), which appears in the contribution of \mathcal{M}_1 to the Z penguin. This happens because, as mentioned before, \mathcal{M}_1 is a singlet of $SU(2)$ and is coupled to Z in the same way as to γ except for the coupling constant. The contributions to the effective γ vertex from F_d and \mathcal{M}_1 will differ from each other in the form of the operators and with x_F and x_M appearing in D_0 respectively. We obtain the following final expressions

$$\mathcal{M}_\gamma^{F,\mu} = \frac{-ie}{16\pi^2} \frac{g_F^2}{4M_F^2} b D_0(x_F) \bar{s}(q^2\gamma^\mu - q^\mu \not{q})(1 - \gamma^5)d + \mathcal{O}(b^2), \quad (32)$$

and

$$\mathcal{M}_\gamma^{\mathcal{M}_1,\mu} = \frac{-ie}{16\pi^2} \frac{g_F^2}{4M_{\mathcal{M}_1}^2} b D_0(x_M) \bar{s}(q^2\gamma^\mu - q^\mu \not{q})(1 + \gamma^5)d + \mathcal{O}(b^2). \quad (33)$$

The corresponding expression for the SM as given in Ref. [4] is

$$\mathcal{M}_\gamma^{SM,\mu} = \frac{-ie}{16\pi^2} \frac{g^2}{4M_W^2} V_{ts}^* V_{td} D_0^{SM}(x_t) \bar{s}(q^2\gamma^\mu - q^\mu \not{q})(1 - \gamma^5)d, \quad (34)$$

with

$$D_0^{SM}(x_t) = -\frac{4}{9} \ln x_t + \frac{-19x_t^3 + 25x_t^2}{36(x_t - 1)^3} + \frac{x_t^2(5x_t^2 - 2x_t - 6)}{18(x_t - 1)^4} \ln x_t. \quad (35)$$

V. THE GLUON EFFECTIVE VERTEX

The function D_0 which appears in the γ vertex also appears in the gluon effective vertex, with the only difference appearing in the prefactor due to the different nature of the charge. This is so because g and γ have vector couplings to the same particles in our model. This does not happen in the SM where γ can couple to W while the gluon cannot. As a result, the number of diagrams in the SM, used to describe the effective vertices, and the functions

that appear in there, are different for the gluon and for γ . We introduce the function E_0 given by

$$E_0 = -3D_0, \quad (36)$$

to absorb the factor $-1/3$ in D_0 coming from the electric charge of the quarks. The final expressions for the contributions to the gluon effective vertex due to F_d and \mathcal{M}_1 are (α, β are color indices and g_s is the $SU(3)_c$ coupling)

$$\mathcal{M}_g^{F,a,\mu} = \frac{ig_s}{16\pi^2} \frac{g_F^2}{4M_F^2} bE_0(x_F) \bar{s}_\alpha (q^2 \gamma^\mu - q^\mu \not{q}) (1 - \gamma^5) T_{\alpha\beta}^a d_\beta + \mathcal{O}(b^2), \quad (37)$$

and

$$\mathcal{M}_g^{\mathcal{M}_1,a,\mu} = \frac{ig_s}{16\pi^2} \frac{g_F^2}{4M_{\mathcal{M}_1}^2} bE_0(x_M) \bar{s}_\alpha (q^2 \gamma^\mu - q^\mu \not{q}) (1 + \gamma^5) T_{\alpha\beta}^a d_\beta + \mathcal{O}(b^2), \quad (38)$$

where $(T_{\alpha\beta})^a$ is the a -th generator of $SU(3)_c$. The corresponding expression for the SM as given in Ref. [4] is

$$\mathcal{M}_{g,SM}^{a,\mu} = \frac{ig_s}{16\pi^2} \frac{g^2}{4M_W^2} V_{ts}^* V_{td} E_0^{SM}(x_t) \bar{s}_\alpha (q^2 \gamma^\mu - q^\mu \not{q}) (1 - \gamma^5) T_{\alpha\beta}^a d_\beta, \quad (39)$$

with

$$E_0^{SM}(x_t) = -\frac{2}{3} \ln x_t + \frac{x_t^2(15 - 16x_t + 4x_t^2)}{6(1 - x_t)^4} \ln x_t + \frac{x_t(18 - 11x_t - x_t^2)}{12(1 - x_t)^3}. \quad (40)$$

Knowing the expressions for the effective vertices in the new model is what we need to derive completely the new contributions to the FCNC processes with $\Delta S = 1$ involving penguin diagrams. These new contributions differ from the corresponding ones in the SM only in the effective vertex.

VI. BOX AMPLITUDES

For the contributions to the FCNC processes with $\Delta S = 1$ coming from box diagrams we have to calculate directly the amplitude. In Fig. 5 we show the new one loop diagrams describing FCNC processes with $\Delta S = 1$ coming from our model. The new contributions

coming from the box diagrams to the FCNC processes with $\Delta S = 1$ are suppressed by the factor $1/M_G^2$. This makes these box contributions negligible with respect to the dominant contribution, due to the Z penguin, which is suppressed only by the factor $1/M_W^2$ coming from the Z propagator. The number of box diagrams is eight, considering only the ones in which the NG bosons propagating in the loop are the $\tilde{\Omega}'_i$. The diagrams in which the pseudo NG bosons $Re\tilde{\rho}'_i$ are propagating in the loop are suppressed by $\sin^4\beta$ while those which contain both NG bosons and pseudo NG bosons are suppressed by $\sin^2\beta$. The first two diagrams (Fig. 5a,b) have the F vector-like particles propagating in the loop. Neglecting terms of order m_q^2/M_G^2 with m_q being the mass of the external quarks, we find the same amplitude for the two diagrams. We also use the identity

$$\begin{aligned} \bar{s}(p_1)\gamma^\mu(1-\gamma^5)d(p_2)\bar{d}(p_4)\gamma_\mu(1-\gamma^5)d(p_3) = \\ \bar{s}(p_1)\gamma^\mu(1-\gamma^5)d(p_3)\bar{d}(p_4)\gamma^\mu(1-\gamma^5)d(p_2), \end{aligned} \quad (41)$$

applying Fierz transformations. For both diagrams the amplitude is given by

$$\mathcal{M}_{box} = \frac{ig_F^4}{16\pi^2 M_G^2} B_0(x_F, b) \bar{s}\gamma^\mu(1-\gamma^5)d \bar{d}\gamma_\mu(1-\gamma^5)d, \quad (42)$$

where $B_0(x_F, b)$ is given by

$$\begin{aligned} B_0(x_F, b) = \frac{-(1+b)^2 + x^2 + 2(1+b)x(\ln(1+b) - \ln(x))}{2(1+b-x)^3} - \\ \frac{-(1-b)^2 + x^2 + 2(1-b)x(\ln(1-b) - \ln(x))}{2(1-b-x)^3}. \end{aligned} \quad (43)$$

For the function $B_0(x_F, b)$, in the same way as for $C_0(x_F, b)$ and $D_0(x_F, b)$, we make a Taylor expansion in the parameter b . Also in this case as in the case for the Z and γ vertices the zeroth order term in the expansion is not present and the first non vanishing term is that one which is linear in b . The amplitude in Eq. 42 now takes the simple form

$$\mathcal{M}_{box} = \frac{ig_F^4}{16\pi^2 M_G^2} b B_0(x_F) \bar{s}\gamma^\mu(1-\gamma^5)d \bar{d}\gamma^\mu(1-\gamma^5)d + \mathcal{O}(b^2), \quad (44)$$

where $B_0(x_F)$ is given by

$$B_0(x_F) = \frac{1 + (4 - 5x) x + 2x(2+x) \ln(x)}{(-1+x)^4}. \quad (45)$$

The amplitudes for the box diagrams in which we substitute the vector-like fermions F with \mathcal{M}_1 have similar expressions except in the operator which now has the form $(V + A)(V + A)$ instead of $(V - A)(V - A)$ and with x_M now appearing in the function B_0 . As in Ref. [3], we expect $M_{\mathcal{M}_1}$ to be much larger than M_F so that $x_M = M_{\mathcal{M}_1}^2/M_G^2$ is closer to unity while $x_F = M_F^2/M_G^2$ can be much less than unity. As can be seen from Fig. 6, B_0 varies by at most an order of magnitude for $0 < x_{F,M} \leq 1$. As a result we expect the contributions of the two diagrams due to \mathcal{M}_1 to be smaller than the corresponding ones due to F by not more than one order of magnitude. For the four box diagrams in which there are one vector-like particle of type F and one of type \mathcal{M}_1 , the analytical expressions are too complicated to be written down in this paper. Instead we perform a numerical evaluation for the function $B_{mix0}(x_F, x_M)$ in the mixed case giving us values between $B_0(x_F)$ and $B_0(x_M)$. The operators for these last four box diagrams are of the form $(V - A)(V + A)$ and $(V + A)(V - A)$.

The amplitude for the box diagrams in the SM [4] is given by

$$\mathcal{M}_{box}^{SM} = \frac{g^4}{64\pi^2 M_W^2} V_{ts}^* V_{td} |V_{td}|^2 B_0^{SM}(x_t) \bar{s} \gamma^\mu (1 - \gamma^5) d \bar{d} \gamma^\mu (1 - \gamma^5) d, \quad (46)$$

where

$$B_0^{SM}(x_t) = \frac{1}{4} \left[\frac{x_t}{1 - x_t} + \frac{x_t \ln x_t}{(x_t - 1)^2} \right]. \quad (47)$$

VII. CONSTRAINT ON b FROM THE UPPER BOUND ON $K_L \rightarrow \mu^+ \mu^-$

From our analysis of the new contributions to FCNC processes with $\Delta S = 1$, it turns out that the main contribution is given by the Z penguin, all the other contributions being $1/M_G^2$ suppressed.

The FCNC processes with $\Delta S = 1$ in kaon physics are reasonably well described by the SM, with uncertainties coming from non perturbative QCD effects. On the other hand

the apparent discrepancy for example between the SM estimates and the data invites for speculations about non standard contributions to ϵ'/ϵ [9], and also for FCNC rare decays there are still margins for effects of new physics [8]. Now in our extension of the SM, the only non negligible contribution comes from the Z penguin and corresponds to the operator $V - A$, the same as in the Z penguin of the SM.

The way we proceed follows Ref. [5], [6]. First of all we write down the effective Lagrangians corresponding to the flavour-changing coupling of the Z boson to down-type quarks in the SM and in our model, looking only, for the latter case, at the dominant contribution. We have

$$\mathcal{L}_Z^{SM} = \frac{g}{16\pi^2 \cos(\theta_W)} g^2 Z_{ds}^{SM} \bar{s} \gamma^\mu (1 - \gamma^5) d Z_\mu + h.c. , \quad (48)$$

with

$$Z_{ds}^{SM} = V_{ts}^* V_{td} C_0^{SM}(x_t) , \quad (49)$$

and

$$\mathcal{L}_Z^F = \frac{-g}{16\pi^2 \cos(\theta_W)} g_F^2 Z_{ds}^F \bar{s} \gamma^\mu (1 - \gamma^5) d Z_\mu + h.c. + \mathcal{O}(b^2) , \quad (50)$$

with

$$Z_{ds}^F = b C_0(x_F) . \quad (51)$$

We notice here that Eq. 48 and 50 are related to Eq. 29 and 22 through the equation

$$\mathcal{L} = -i\mathcal{M}^\mu Z_\mu + h.c. . \quad (52)$$

As showed in Ref. [5] the coupling Z_{ds}^{SM} is complex, being the product of the quantity $V_{ts}^* V_{td}$, which is complex, where V_{ij} are elements of the CKM matrix, and the function $C_0(x_t)$ which is real. In particular, from the standard analysis of the unitary triangle, one has

$$Im(V_{ts}^* V_{td}) = (1.38 \pm 0.33) \cdot 10^{-4} , \quad (53)$$

$$Re(V_{ts}^* V_{td}) = -(3.2 \pm 0.9) \cdot 10^{-4} , \quad (54)$$

which, using for $C_0(x_t)$ the value of 0.79 corresponding to the central value of the top quark mass, $\bar{m}_t(m_t) = 166 \text{ GeV}$, give

$$\text{Im}Z_{ds}^{SM} = (1.09 \pm 0.26) \cdot 10^{-4}, \quad (55)$$

$$\text{Re}Z_{ds}^{SM} = -(2.54 \pm 0.71) \cdot 10^{-4}. \quad (56)$$

The complex nature of the coupling Z_{ds}^{SM} is responsible for CP violation in the SM, as can be verified by looking at the expression for ϵ'/ϵ as given in Ref. [5]:

$$\frac{\epsilon'}{\epsilon} = \left(\frac{\epsilon'}{\epsilon}\right)_Z + \left(\frac{\epsilon'}{\epsilon}\right)_{Rest}, \quad (57)$$

where

$$\left(\frac{\epsilon'}{\epsilon}\right)_Z = \text{Im}Z_{ds} \left[1.2 - R_s |r_Z^{(8)}| B_8^{(3/2)}\right], \quad (58)$$

and

$$\left(\frac{\epsilon'}{\epsilon}\right)_{Rest} = \text{Im}(V_{ts}^* V_{td}) \left[-2.3 + R_s \left[1.1 |r_Z^{(8)}| B_6^{(1/2)} + (1.0 + 0.12 |r_Z^{(8)}|) B_8^{(3/2)}\right]\right], \quad (59)$$

which is proportional to $\text{Im}(V_{ts}^* V_{td})$. All the parameters appearing in the above expressions are fully described in Ref. [5]. As pointed out in Ref. [5], if we assume that no new operators in addition to those present in the SM contribute, and this is true in the approximation of neglecting the new contributions which are suppressed by the factor $1/M_G^2$, the replacement $Z_{ds}^{SM} \rightarrow Z_{ds}$, where

$$Z_{ds} = Z_{ds}^{SM} + \frac{g_F^2}{g^2} Z_{ds}^F, \quad (60)$$

a relation that holds separately for $\text{Re}Z_{ds}$ and $\text{Im}Z_{ds}$

$$\text{Re}Z_{ds} = \text{Re}Z_{ds}^{SM} + \frac{g_F^2}{g^2} \text{Re}Z_{ds}^F, \quad (61)$$

$$\text{Im}Z_{ds} = \text{Im}Z_{ds}^{SM} + \frac{g_F^2}{g^2} \text{Im}Z_{ds}^F, \quad (62)$$

which is justified without the modification of QCD renormalization group effects evaluated at NLO level for scales below $\mathcal{O}(m_t)$. This means that to look at the effects of new physics,

described by a modified effective coupling of the Z boson to down-type quarks, to the quantity ϵ'/ϵ , we just need to substitute ImZ_{ds} to ImZ_{ds}^{SM} in Eq. 58. Looking at Eq. 51, Z_{ds}^F is the product of the parameter b , introduced in Eq. 16, which has been chosen real and the function $C_0(x_F)$, which is also real making Z_{ds}^F real. This implies that in our model there are no corrections to ImZ_{ds}^{SM} and consequently to ϵ'/ϵ . Obviously this means that we cannot use the experimental results on ϵ'/ϵ to constrain the parameter b . As shown in Ref. [5], if new physics affects ReZ_{ds} , as it is the case in our model, the process to look at to reveal effects of new physics is the FCNC decay $K_L \rightarrow \mu^+\mu^-$, whose experimental branching ratio $BR(K_L \rightarrow \mu^+\mu^-) = (7.2 \pm 0.5) \cdot 10^{-9}$ [12]. The effects of new physics appear in the short-distance (SD) contribution to $BR(K_L \rightarrow \mu^+\mu^-)$

$$BR(K_L \rightarrow \mu^+\mu^-)_{SD} = 6.32 \cdot 10^{-3} \left[ReZ_{ds} - B_0 Re(V_{ts}^* V_{td}) + \bar{\Delta}_c \right]^2, \quad (63)$$

where $B_0 = -0.182$ is the box diagram function evaluated at $\bar{m}_t(m_t) = 166 GeV$, and

$$\bar{\Delta}_c = -(6.54 \pm 0.60) \cdot 10^{-5}, \quad (64)$$

represents the charm contribution [11]. From the analysis in Ref. [5] of the long distance (LD) and SD contributions to $BR(K_L \rightarrow \mu^+\mu^-)$ the highest possible value for $BR(K_L \rightarrow \mu^+\mu^-)_{SD}$ is derived

$$BR(K_L \rightarrow \mu^+\mu^-)_{SD} < 2.8 \cdot 10^{-9}. \quad (65)$$

Now using Eq. 65 together with Eq. 60, 56 and 51 we obtain the following upper bound on the parameter b

$$b < 2.5 \cdot 10^{-4}, \quad (66)$$

where in Z_{ds}^F we have used $C_0(10^{-6}) \simeq 0.5$ which corresponds to $M_F = 200 GeV$ and $M_G = 200 TeV$, and in Z_{ds} we have used $g = 0.65$ and $g_F = 1$.

Looking at the expressions for $BR(K_L \rightarrow \pi^0 \nu \bar{\nu})$, $BR(K_L \rightarrow \pi^0 e^+ e^-)$ and $BR(K^+ \rightarrow \pi^+ \nu \bar{\nu})$ given in Ref. [5], we observe that there are no new contributions from our model

to the first two decays, which depend only on ImZ_{ds} , while there is a contribution to $K^+ \rightarrow \pi^+ \nu \bar{\nu}$, which depends also on ReZ_{ds} . In Ref. [5], the expression for the upper bound on $BR(K^+ \rightarrow \pi^+ \nu \bar{\nu})$ is given in terms of $BR(K_L \rightarrow \pi^0 \nu \bar{\nu})$, and the parameter κ related to $BR(K_L \rightarrow \mu^+ \mu^-)_{SD}$ by the relation

$$BR(K_L \rightarrow \mu^+ \mu^-)_{SD} = \kappa \cdot 10^{-9}. \quad (67)$$

Now, if as in Ref. [5] we use the upper bound for $BR(K_L \rightarrow \mu^+ \mu^-)_{SD}$ given in Eq. 65, we obtain

$$BR(K^+ \rightarrow \pi^+ \nu \bar{\nu}) < 0.229 \cdot BR(K_L \rightarrow \pi^0 \nu \bar{\nu}) + 1.76 \cdot 10^{-10}, \quad (68)$$

while, if we use the upper theoretical value for the $BR(K_L \rightarrow \mu^+ \mu^-)_{SD}^{SM}$ given in Ref. [5], we obtain

$$BR(K^+ \rightarrow \pi^+ \nu \bar{\nu}) < 0.229 \cdot BR(K_L \rightarrow \pi^0 \nu \bar{\nu}) + 1.15 \cdot 10^{-10}. \quad (69)$$

In Ref. [5], for the particular scenario in which all the effects of new physics are encoded in the effective coupling Z_{ds} , $BR(K_L \rightarrow \pi^0 \nu \bar{\nu})$ is estimated to range in the interval $(1.3 \cdot 10^{-10}, 2.4 \cdot 10^{-10})$ for $B_8^{(3/2)} = 0.6$, and this makes the contribution due to the maximum value for $BR(K_L \rightarrow \mu^+ \mu^-)_{SD}$ in the expression for the upper bound of $BR(K^+ \rightarrow \pi^+ \nu \bar{\nu})$ the dominant contribution. The difference between the two upper bounds for $BR(K^+ \rightarrow \pi^+ \nu \bar{\nu})$ shows the room for a possible contribution of new physics associated to the quantity ReZ_{ds} .

Using the constraint on b derived in Eq. 66, we can now check if the amplitudes that we know to be $1/M_G^2$ suppressed are negligible with respect to the corresponding SM amplitudes. In the case of the photon, matching the absolute value of the functions which multiplies the $V - A$ operator for the new amplitude and the SM one, we have, after cancelling out all the common factors,

$$\frac{M_W^2}{M_F^2} \left| \frac{g_F^2 b D_0(x_F)}{g^2 Re(V_{ts}^* V_{td}) D_0^{SM}(x_t)} \right| \leq 1.7 \cdot 10^{-6}, \quad (70)$$

where we have used $D_0(10^{-6}) \simeq -2.66 \cdot 10^{-6}$, and for the SM quantities $D_0^{SM}(4.27) \simeq -0.46$, $Re(V_{ts}^* V_{td})$ as given in Eq. 54, and obviously the constraint on b from Eq. 66.

In the case of the gluon we have

$$\frac{M_W^2}{M_F^2} \left| \frac{g_F^2 b E_0(x_F)}{g^2 \text{Re}(V_{ts}^* V_{td}) E_0^{SM}(x_t)} \right| \leq 8.7 \cdot 10^{-6}, \quad (71)$$

where we have used $E_0^{SM}(4.27) \simeq 0.27$. From what we have seen above, the amplitudes with the $V - A$ operator for the photon and for the gluon, which have corresponding ones in the SM, are negligible. Now the amplitudes with the $V + A$ operator which appears in our model, and are present in the effective vertices for the Z , the photon and the gluon, are also $1/M_G^2$ suppressed and are not relevant.

For the box diagrams, we look at the function which multiplies the $(V - A)(V - A)$ operator. We obtain the ratio

$$\frac{M_W^2}{M_G^2} \left| \frac{4g_F^4 b B_0(x_F)}{g^4 \text{Re}(V_{ts}^* V_{td}) |V_{td}|^2 B_0^{SM}(x_t)} \right| \leq 0.19, \quad (72)$$

where we have used $B_0(10^{-6}) \simeq 1$ and for the SM quantities $B_0^{SM}(4.27) \simeq -0.18$ and $|V_{td}| \simeq 9.1 \cdot 10^{-3}$. Similarly, the amplitudes containing the operators $(V + A)(V + A)$, $(V - A)(V + A)$ and $(V + A)(V - A)$ are also not relevant. It is important to notice here that, for the box diagrams, the $1/M_G^2$ suppression of the new contribution is balanced by the $|V_{td}|^2$ suppression of the SM one.

In Ref. [3] it has been shown in two numerical examples how it is possible to derive the neutrino mass splittings Δm_{32}^2 and Δm_{21}^2 for different values of b . In fact, in Ref. [3], b has been introduced as a free parameter chosen to be smaller than unity. In this paper it has been shown how it is possible to constrain the parameter b by looking at the quark sector. In accordance with the upper bound for b derived in this paper and presented in Eq. 66, we give here the neutrino mass splittings obtained numerically in Ref. [3] for the particular choice of the parameter $b = 0.000095$

$$\Delta m_{32}^2 = 2.02 \cdot 10^{-3} eV^2, \quad (73)$$

$$\Delta m_{21}^2 = 5.497 \cdot 10^{-6} eV^2. \quad (74)$$

It is important to notice here that, when one chooses a particular value of the parameter b , one also has to choose the internal loop variables which appear in the function given in Eq. 92, in order to reproduce the mass splittings of Eq. 73 and 74. This means, as one can see from the two numerical examples with different values of the parameter b in Ref. [3], that different values of b will correspond to different sets of masses for the three light neutrinos.

VIII. OTHER RARE KAON DECAYS BEYOND THE SM

Being sensitive to flavour dynamics from few MeV up to several TeV, rare kaon decays provide a powerful tool to test the SM and to search for new physics. Decays like $K_L \rightarrow \mu e$ and $K_L \rightarrow \pi \mu e$ are completely forbidden within the SM [8], where lepton flavour is conserved, and are also absolutely negligible if we simply extend the model by including Dirac type neutrino masses with the standard Yukawa mass term.

In our model the neutrinos are still only Dirac, but the way they get masses is through loop diagrams, and processes like $K_L \rightarrow \mu e$ or $K_L \rightarrow \pi \mu e$ are made possible through the exchange of virtual NG bosons $\tilde{\Omega}'_i$. They, in fact, as we have already said, can couple to different flavours and, in the way we build our model, are the same for the lepton and the quark sectors.

In the following, we will calculate explicitly the branching ratio for the decay $K_L \rightarrow \mu e$ in our model, and we will give a theoretical range of values corresponding to different values for the mass of the vector-like fermions $M_{\mathcal{M}_1^{l,q}}$.

This decay happens through five diagrams, shown in Fig. 8: four box diagrams that have to be considered with their corresponding crossed diagrams, and the diagram obtained by linking two effective Z vertexes by a virtual Z . It can be shown that the crossed diagrams are b suppressed with respect to the ones shown in Fig. 8. The diagram where the virtual Z is exchanged is also b suppressed, but not $1/M_G^2$ suppressed as the surviving box diagrams and so we will expect the sum of all the contributions will depend on the values of the

parameters b and M_G . The final amplitude for the process $K_L \rightarrow \mu e$ is given by

$$\begin{aligned} \mathcal{M} = \frac{ig_F^2}{2M_G^2} & \left[\left(\frac{g_F^2}{4\pi^2} B(x_{F_q}, x_{F_l}, b) - \frac{g^2 g_F^2 M_G^2}{32\pi^4 M_Z^2 \cos^2(\theta_W)} b^2 C_0(x_{F_q}) C_0(x_{F_l}) \right) \bar{s} \gamma^\mu P_L d \bar{e} \gamma_\mu P_L \mu \right. \\ & + \frac{g_F^2}{4\pi^2} B(x_{F_q}, x_{M_l}, b) \bar{s} \gamma^\mu P_L d \bar{e} \gamma_\mu P_R \mu \\ & + \frac{g_F^2}{4\pi^2} B(x_{M_q}, x_{F_l}, b) \bar{s} \gamma^\mu P_R d \bar{e} \gamma_\mu P_L \mu \\ & \left. + \frac{g_F^2}{4\pi^2} B(x_{M_q}, x_{M_l}, b) \bar{s} \gamma^\mu P_R d \bar{e} \gamma_\mu P_R \mu \right], \end{aligned} \quad (75)$$

with B being the function coming from the box diagrams (which is too long to be written down explicitly in this paper), C_0 given in Eq. 21, and $P_{L,R} = \frac{1 \mp \gamma^5}{2}$. To obtain the BR we can use the expression given in ref. [7] for our case

$$BR = 11.24 \cdot 10^{-12} \left[\frac{g_F}{g} \frac{100 \text{TeV}}{M_G} \right]^4 (C_{Lq} - C_{Rq})^2 (C_{Ll}^2 + C_{Rl}^2), \quad (76)$$

that for our purpose can be rewritten as:

$$\begin{aligned} BR = 11.24 \cdot 10^{-12} & \left[\frac{g_F}{g} \frac{100 \text{TeV}}{M_G} \right]^4 [(C_{Lq} C_{Ll})^2 + (C_{Lq} C_{Rl})^2 + (C_{Rq} C_{Ll})^2 + (C_{Rq} C_{Rl})^2 \\ & - 2(C_{Lq} C_{Ll})(C_{Rq} C_{Ll}) - 2(C_{Lq} C_{Rl})(C_{Rq} C_{Rl})], \end{aligned} \quad (77)$$

where $C_{Lq}, C_{Rq}, C_{Ll}, C_{Rl}$ appear in the expression for the operator $\mathcal{O}_{V,A}$

$$\mathcal{O}_{V,A} = \frac{g_F^2}{2M_G^2} \bar{s} \gamma^\mu [C_{Lq} P_L + C_{Rq} P_R] d \bar{e} \gamma_\mu [C_{Ll} P_L + C_{Rl} P_R] \mu + h.c.. \quad (78)$$

From the way we have written the amplitude \mathcal{M} in Eq. 75 it is possible to isolate the four contributions $C_{Lq} C_{Ll}$, $C_{Lq} C_{Rl}$, $C_{Rq} C_{Ll}$ and $C_{Rq} C_{Rl}$ that appear in Eq. 77.

$$\begin{aligned} C_{Lq} C_{Ll} &= \frac{g_F^2}{4\pi^2} B(x_{F_q}, x_{F_l}, b) - \frac{g^2 g_F^2 M_G^2}{32\pi^4 M_Z^2 \cos^2(\theta_W)} b^2 C_0(x_{F_q}) C_0(x_{F_l}), \\ C_{Lq} C_{Rl} &= \frac{g_F^2}{4\pi^2} B(x_{F_q}, x_{M_l}, b), \\ C_{Rq} C_{Ll} &= \frac{g_F^2}{4\pi^2} B(x_{M_q}, x_{F_l}, b), \\ C_{Rq} C_{Rl} &= \frac{g_F^2}{4\pi^2} B(x_{M_q}, x_{M_l}, b). \end{aligned} \quad (79)$$

In Fig. 9, the logarithm of the quantity $(C_{Lq} - C_{Rq})^2 (C_{Ll}^2 + C_{Rl}^2)$ is plotted as a function of the logarithm of the ratio x_M/x_F , with $M_G = 200 \text{TeV}$, $x_F = 10^{-6}$ and using for b the

upper bound given in Eq. 66, so that the contribution coming from the diagram with the virtual Z has its highest value. In doing the plot of Fig. 9 we have also chosen $M_{\mathcal{M}_1^l} = M_{\mathcal{M}_1^q}$ and $M_{F^l} = M_{F^q} = 200\text{GeV}$. In Fig. 10 the logarithm of $BR(K_L \rightarrow \mu e)$ is plotted as a function of the logarithm of the ratio x_M/x_F , for the same values of the quantities M_G , x_F and b as in Fig. 9, and the same choice $M_{\mathcal{M}_1^l} = M_{\mathcal{M}_1^q}$ and $M_{F^l} = M_{F^q} = 200\text{GeV}$. It can be seen from Fig. 10 that $BR(K_L \rightarrow \mu e)$ depends strongly on x_M , starting from $6.65 \cdot 10^{-22}$ for $x_M/x_F = 1$, and reaching the asymptotic value of $1.02 \cdot 10^{-14}$. It is important to notice here that the lowest value for $BR(K_L \rightarrow \mu e)$, when $x_M/x_F = 1$, corresponds to the situation in which the contributions of the box diagrams cancel out and the only contribution left is due to the diagram with the virtual Z . In this case we have

$$\begin{aligned} BR(K_L \rightarrow \mu e) &= 11.24 \cdot 10^{-12} \left[\frac{g_F}{g} 100\text{TeV} \right]^4 \left(\frac{g^2 g_F^2}{32\pi^4 M_Z^2 \cos^2(\theta_W)} b^2 C_0(x_{F_q}) C_0(x_{F_l}) \right)^2 \\ &= 6.65 \cdot 10^{-22}, \end{aligned} \quad (80)$$

where we have used for b the upper bound given in Eq. 66. The asymptotic value for $BR(K_L \rightarrow \mu e)$, when $x_M/x_F \gg 1$, corresponds instead to the situation in which the box diagram with F^l and F^q propagating in the loop, gives the dominant contribution, and all the contributions from the other diagrams, including the one from the Z penguin, are negligible. In this case we have

$$BR = 11.24 \cdot 10^{-12} \left[\frac{g_F}{g} \frac{100\text{TeV}}{M_G} \right]^4 (C_{Lq} C_{Ll})^2 = 1.02 \cdot 10^{-14}, \quad (81)$$

which is independent of b .

The range of values for $BR(K_L \rightarrow \mu e)$ agrees with the actual experimental upper bound of $3 \cdot 10^{-12}$ at 90 % CL [10]. This range is however quite wide, spanning eight orders of magnitude, and is due to the fact that the branching ratio has a strong dependence on the masses of the vector-like fermions $F^{l,q}$ and $\mathcal{M}_1^{l,q}$. Notice from Table 1 that $F^{l,q}$ are the vector-like leptons and quarks which are $SU(2)_L$ doublets, while $\mathcal{M}_1^{l,q}$ denotes an $SU(2)_L$ singlet charged lepton and quark respectively. It is interesting to note from Fig. 10 that, in the case where all vector-like fermions are in the interesting mass range (a few hundreds

of GeV's) where they can be produced by QCD or Electroweak processes, $BR(K_L \rightarrow \mu e)$ is hopelessly small to have a chance to be observed (the lower flat part of Fig. 10). At the other extreme (the upper flat part of Fig. 10), $BR(K_L \rightarrow \mu e) \sim 10^{-14}$ while the mass of $\mathcal{M}_1^{l,q}$ is unreachable (of O(few hundreds TeV's) assuming the mass of $F^{l,q}$ is of order a few hundreds of GeV's) by any conceivable earthbound machine.

IX. EPILOGUE

We have presented a link between the quark sector and the lepton sector based on a model of neutrino masses [3]. This link manifests itself in a common (small) parameter, b , which appears in both sectors. In the neutrino sector, b is crucial in determining the magnitude of the mass splitting Δm^2 , and, in an indirect manner, the masses themselves. In fact, the model presented in Ref. [3] deals with the case of three light, degenerate neutrinos, and the lifting of this degeneracy is proportional to b . In the quark sector, as we have seen above, this same parameter appears in various FCNC penguin operators which are seen to be linear in b at the lowest order. It is well-known that these penguin operators are important in various aspects of Kaon physics: ϵ'/ϵ , rare K decays, etc... Strong constraints in this sector would also constrain the neutrino sector as well. It turns out, as we have shown above, that there is no contribution to ϵ'/ϵ from our model, to lowest order in b . However, at the same order in b , our model makes a contribution to the rare decay process $K_L \rightarrow \mu^+ \mu^-$. Taking into account the upper bound on the short distance contribution to that process, we found a strong constraint on b which is $b < 2.5 \times 10^{-4}$.

We have also calculated the $BR(K_L \rightarrow \mu e)$, finding that it strongly depends on the masses of the vector-like fermions $F^{l,q}$ and $\mathcal{M}_1^{l,q}$ and on b for a certain range of those masses. We found that $BR(K_L \rightarrow \mu e)$ goes from $6.65 \cdot 10^{-22}$ which makes this decay practically unobservable, to $1.02 \cdot 10^{-14}$, with the choice of $M_G = 200 \text{ TeV}$ and $x_F = 10^{-6}$, when x_M/x_F goes from 1 to 10^{12} . For b we have used the upper bound derived from $K_L \rightarrow \mu^+ \mu^-$. As one can see from Fig. 10, the first case ($6.65 \cdot 10^{-22}$) corresponds to the interesting situation

where it might be possible to produce and observe these vector-like particles since their masses could lie in the few-hundred GeV region [13], despite the fact that one will not be able to observe $K_L \rightarrow \mu e$. The second case ($1.02 \cdot 10^{-14}$) corresponds to a possible observation for $K_L \rightarrow \mu e$, while forsaking that of the singlet quark and charged lepton $\mathcal{M}_1^{l,q}$. And finally, there are these in-between cases as can be seen from Fig. 10.

Because of the upper limit on b , and obviously because of the choice of heavy family gauge bosons, M_G of $\mathcal{O}(100\text{TeV})$, it turns out that the physics of the kaon sector by itself, in our model, is not too different from the SM. Nevertheless, we have seen that there is still some margin for possible contributions of new physics to $K_L \rightarrow \mu^+ \mu^-$, the bound on $K^+ \rightarrow \pi^+ \nu \bar{\nu}$. As for the decay $K_L \rightarrow \mu e$, which is forbidden in the SM, we have seen that our model can make a non-negligible contribution ($BR \sim 10^{-14}$) which is practically independent of b . In the region where it depends strongly on b (the lower flat region of Fig. 10), the branching ratio is negligible, practically similar to the SM with a Dirac neutrino. In that region, as we have stressed above, the new physics signal would be the production and observation of the vector-like fermions.

The bound on b could have interesting implications on the neutrino sector itself, as we have mentioned above. It was shown in Ref. [3] how the parameter b affects the mass splitting of three formerly degenerate neutrinos. In particular, it was shown how Δm^2 is sensitive to b . However, it was also shown how b indirectly affects the overall magnitude of the masses. Unfortunately, at the present time, one is quite far experimentally from a direct determination of the masses themselves. Needless to say, future experiments are of paramount importance to this crucial question.

ACKNOWLEDGMENTS

This work is supported in parts by the US Department of Energy under grant No. DE-A505-89ER40518 (PQH), and by the Italian INFN Fellowship (AS).

X. APPENDIX A

In this appendix, we will summarize the results of Ref. [3]. The Yukawa part of the Lagrangian involving leptons can be written as

$$\begin{aligned} \mathcal{L}_{Lepton}^Y = & g_E \bar{l}_L^\alpha \phi e_{\alpha R} + G_1 \bar{l}_L^\alpha \Omega_\alpha F_R + G_{\mathcal{M}_1} \bar{F}_L \phi \mathcal{M}_{1R} + G_{\mathcal{M}_2} \bar{F}_L \tilde{\phi} \mathcal{M}_{2R} + G_2 \bar{\mathcal{M}}_{1L} \Omega_\alpha e_R^\alpha + \\ & G_3 \bar{\mathcal{M}}_{2L} \rho_m^\alpha \eta_{\alpha R}^m + M_F \bar{F}_L F_R + M_{\mathcal{M}_1} \bar{\mathcal{M}}_{1L} \mathcal{M}_{1R} + M_{\mathcal{M}_2} \bar{\mathcal{M}}_{2L} \mathcal{M}_{2R} + h.c.. \end{aligned} \quad (82)$$

which, after integrating out the vector-like fermions F , \mathcal{M}_1 and \mathcal{M}_2 , brings to the effective Lagrangian

$$\begin{aligned} \mathcal{L}_{Lepton}^{Y,eff} = & g_E \bar{l}_L^\alpha \phi e_{\alpha R} + G_E \bar{l}_L^\alpha (\Omega_\alpha \phi \Omega^\beta) e_{\beta R} + \\ & G_N \bar{l}_L^\alpha (\Omega_\alpha \tilde{\phi} \rho_i^\beta) \eta_{\beta R}^i + h.c., \end{aligned} \quad (83)$$

where

$$G_E = \frac{G_1 G_{\mathcal{M}_1} G_2}{M_F M_{\mathcal{M}_1}}; \quad G_N = \frac{G_1 G_{\mathcal{M}_2} G_3}{M_F M_{\mathcal{M}_2}}. \quad (84)$$

The main assumption in building the above Lagrangian is the conservation of lepton number L , thereby forbidding the presence of Majorana mass terms. The way $\langle \Omega \rangle = (0, 0, 0, V)$ and $\langle \rho \rangle = (0, 0, 0, V' \otimes s_1)$, with $s_1 = \begin{pmatrix} 1 \\ 0 \end{pmatrix}$, have been chosen, makes the neutrino of the 4th family massive at tree level, while the others three neutrino remain massless. These three neutrinos would get a mass dynamically via loop diagrams. For the neutrino of the 4th family we have

$$m_N = G_1 G_{\mathcal{M}_2} G_3 \frac{V V'}{M_F M_{\mathcal{M}_2}} \frac{v}{\sqrt{2}}, \quad (85)$$

which, for

$$V V' / M_F M_{\mathcal{M}_2} \sim O(1), \quad (86)$$

can be expected to be even as heavy as $175 GeV$, satisfying the bound of $M_Z/2$ from LEP.

For the three light neutrinos, one has

$$m_\nu = m_N \frac{M_F M_{\mathcal{M}_2}}{V V'} \frac{\sin(2\beta)}{32 \pi^2} \Delta I(G, P), \quad (87)$$

where $\Delta I(G, P)$ is given by

$$\Delta I(G, P) = \frac{1}{M_F - M_{\mathcal{M}_2}} \left\{ \frac{M_F [M_F^2 (M_G^2 \ln(\frac{M_G^2}{M_F^2}) - M_P^2 \ln(\frac{M_P^2}{M_F^2})) + M_G^2 M_P^2 \ln(\frac{M_P^2}{M_G^2})]}{(M_G^2 - M_F^2)(M_P^2 - M_F^2)} - (M_F \leftrightarrow M_{\mathcal{M}_2}) \right\}. \quad (88)$$

The main result that was obtained in Ref. [3] is that one can obtain for m_ν a value of the $\mathcal{O}(eV)$, or equivalently the ratio $R = m_\nu/m_N \sim \mathcal{O}(10^{-11})$ as long as the ratios of masses of the particles propagating in the loop satisfy certain relations. In Ref. [3] it has been shown that, taking the masses in units of M_F , where M_F could be of $\mathcal{O}(\geq 200 GeV)$, one obtains $R \lesssim 10^{-11}$ for $M_G/M_{\mathcal{M}_2} \lesssim 10^{-3}$ when $M_G \lesssim 10^5$, or for $M_G/M_{\mathcal{M}_2} \sim 10^{-2} - 10^{-1}$ when $M_G > 10^7$, with $M_P \sim 1 - 10^2$. After lifting the degeneracy of the three light neutrinos, by breaking the remaining family symmetry $SO(3)$, one obtains the following mass eigenvalues for the three light neutrinos

$$m_1 = m_N \frac{\sin(2\beta)}{32 \pi^2} \{ \Delta I(G, P) - b \Delta I(G, P, b) \}, \quad (89)$$

$$m_2 = m_N \frac{\sin(2\beta)}{32 \pi^2} \Delta I(G, P), \quad (90)$$

$$m_3 = m_N \frac{\sin(2\beta)}{32 \pi^2} \{ \Delta I(G, P) + b \Delta I(G, P, -b) \}, \quad (91)$$

where $\Delta I(G, P, \pm b)$ is given by

$$\Delta I(G, P, \pm b) \equiv I(M_G, \pm b) - I(M_P, \pm b), \quad (92)$$

with

$$I(M_G, \pm b) = \frac{M_G^2}{M_F - M_{\mathcal{M}_2}} \left\{ \frac{M_F [-M_F^2 (1 \pm b + \ln(\frac{M_G^2}{M_F^2})) + M_G^2 (1 \pm b)]}{(M_G^2 - M_F^2)^2 (1 \pm b (M_G^2 / (M_G^2 - M_F^2)))} - (M_F \leftrightarrow M_{\mathcal{M}_2}) \right\}. \quad (93)$$

The mass splittings, neglecting terms of order b^2 are now

$$m_3^2 - m_2^2 = m_2 m_N 2b \frac{\sin(2\beta)}{32\pi^2} \Delta I(G, P, -b), \quad (94)$$

$$m_2^2 - m_1^2 = m_2 m_N 2b \frac{\sin(2\beta)}{32\pi^2} \Delta I(G, P, b). \quad (95)$$

The above mass splittings are almost degenerate and in Ref. [3] a possible solution to lift this degeneracy was presented. What has been showed is that if one introduces mixing terms in the neutrino mass matrix between the three light families and the 4th family, one can obtain reasonable values for the mass splittings. Two numerical examples have been presented. The mass splittings for the particular choice of the parameter $b = 0.000095$ that satisfies the upper constraint for b derived in this paper and presented in Eq. 66 are given in Eq. 73 and 74.

XI. APPENDIX B

In the following we will show in a simple example how the dependence on the parameter b , introduced in Eq. 16, for the amplitude of the FCNC processes in our model appears. This example will be introduced in an analogous fashion to a FCNC process in the SM, which we know to be governed by the GIM mechanism. The process that we are considering is $t \rightarrow cW^+W^-$. Now the amplitude of this process is proportional to the quantity

$$\sum_{j=d,s,b} V_{tj}^* V_{cj} \frac{1}{p^2 - m_j^2}, \quad (96)$$

where the sum appears because one has to consider all possible virtual down-quarks, and p is the momentum of the virtual quarks. Notice that Eq. 96 represents the approximation $p \gg m_j$ which is a valid one as we shall see below. V_{ij} is the CKM matrix and the unitarity of this matrix implies in particular the relation

$$\sum_{j=d,s,b} V_{tj}^* V_{cj} = 0. \quad (97)$$

Using the above relation we can write Eq. 96 as

$$- \sum_{j=s,b} V_{tj}^* V_{cj} \frac{1}{p^2 - m_d^2} + \sum_{j=d,s,b} V_{tj}^* V_{cj} \frac{1}{p^2 - m_j^2} = \sum_{j=d,s,b} V_{tj}^* V_{cj} \frac{m_j^2 - m_d^2}{(p^2 - m_d^2)(p^2 - m_j^2)}. \quad (98)$$

Using now the approximation

$$V_{ts}^* V_{cs} \simeq -V_{tb}^* V_{cb} \approx -\theta^2, \quad (99)$$

and doing the sum we can rewrite Eq. 96 as

$$\theta^2 \frac{m_b^2 - m_s^2}{(p^2 - m_s^2)(p^2 - m_b^2)}. \quad (100)$$

From kinematic considerations p^2 falls in the range

$$(M_W + m_c)^2 < p^2 < (m_t - M_W)^2, \quad (101)$$

which means that p^2 is of order of M_W^2 . One obtains the final expression

$$\theta^2 \frac{m_b^2}{M_W^2} \frac{1}{p^2 - m_b^2}, \quad (102)$$

which shows the characteristic term of the GIM mechanism m_b^2/M_W^2 for FCNC processes involving external t .

Now, looking at our model, and assume that the process $t \rightarrow cF\mathcal{M}_1$ can kinematically occur, (although it cannot be in reality because $M_F \geq 200\text{GeV}$ and $M_{\mathcal{M}_1} \geq M_F$). The amplitude will be proportional to

$$\sum_j A_{\Omega,j3} A_{\Omega,2j}^T \frac{1}{k^2 - M_{\Omega_j}^2}, \quad (103)$$

where A_Ω is a unitary matrix given by (see Ref. [3])

$$A_\Omega = \begin{pmatrix} \frac{1}{2} & \frac{1}{\sqrt{2}} & \frac{1}{2} \\ \frac{1}{2} & -\frac{1}{\sqrt{2}} & \frac{1}{2} \\ -\frac{1}{\sqrt{2}} & 0 & \frac{1}{\sqrt{2}} \end{pmatrix}, \quad (104)$$

chosen different from that one given in Eq. 7 because otherwise we will have no transition from top to charm, and the sum comes out from the fact that we have to consider as virtual

states any gauge boson of $SO(3)$. The unitarity of the matrix A_Ω implies the particular relation

$$\sum_j A_{\Omega,j3} A_{\Omega,2j}^T = 0, \quad (105)$$

that we can use to rewrite the amplitude as

$$- \sum_{j=2,3} A_{\Omega,j3} A_{\Omega,2j}^T \frac{1}{k^2 - M_{\Omega_1}^2} + \sum_{j=2,3} A_{\Omega,j3} A_{\Omega,2j}^T \frac{1}{k^2 - M_{\Omega_j}^2}, \quad (106)$$

in the same way as we did for the SM. Now for the particular matrix A_Ω that we have chosen, we obtain

$$\begin{aligned} A_{\Omega,23} A_{\Omega,22}^T &= -\frac{1}{2\sqrt{2}}, \\ A_{\Omega,33} A_{\Omega,23}^T &= 0, \end{aligned} \quad (107)$$

which gives

$$-\frac{1}{2\sqrt{2}} \frac{M_{\Omega_2}^2 - M_{\Omega_1}^2}{(k^2 - M_{\Omega_1}^2)(k^2 - M_{\Omega_2}^2)}. \quad (108)$$

Substituting for $M_{\Omega_1}^2$ and $M_{\Omega_2}^2$ the expressions given in Eq. 16 we obtain

$$\frac{1}{\sqrt{2}} \frac{b M_G^2}{(k^2 - M_G^2(1+b))(k^2 - M_G^2(1-b))}. \quad (109)$$

From kinematical considerations we have the following constraints for k^2

$$(m_c + M_{M_1})^2 < k^2 < (m_t - M_F)^2, \quad (110)$$

which implies $k^2 \ll M_G^2$, with $M_{M_1}^2, M_F^2 \ll M_G^2$. The final expression becomes

$$\frac{1}{\sqrt{2}} \frac{b}{k^2 - M_G^2}, \quad (111)$$

which shows the linear dependence on the parameter b . One notices that the linear dependence on the parameter b comes out in the same way as the linear dependence on the quantity m_b^2/M_W^2 in the GIM mechanism of the SM. It is important to notice here that, in the SM, the GIM suppression comes from two factors: the appropriate product of CKM elements and the ratio m_q^2/m_W^2 , where m_q is a quark mass (up or down). (Even if $m_q^2/m_W^2 \sim \mathcal{O}(1)$ such as for the top quark, the CKM suppression factor can be very small.) In our case, the amplitude is always suppressed by the parameter b .

REFERENCES

* e-mail: pqh@virginia.edu .

* e-mail: as7yf@virginia.edu

- [1] Super-Kamiokande collaboration, Phys. Rev. Lett. **81**, 1562 (1998).
- [2] V. Fanti et al., Phys Lett. **B465**, 335 (1999); A. Alavi-Harati et al., Phys. Rev. Lett. **83**, 22 (1999).
- [3] P. Q. Hung, Phys. Rev. **D62**, 053015 (2000).
- [4] A. J. Buras, hep-ph/9806471, in *Probing the Standard Model of Particle Interactions*, F. David and R. Gupta, edited by Elsevier Science B. V., 1998.
- [5] A. J. Buras, L. Silvestrini, Nucl. Phys. **B546**, 299 (1999).
- [6] L. Silvestrini, hep-ph/9906202, in *Proceedings of the 34th rencontres de Moriond: Electroweak Interactions and united theories*, Les Arcs, France 13-20 Mar 1999, edited by J. Tran Thanh Van.
- [7] T.G. Rizzo, hep-ph/9809526, in *Proceedings of Workshop on CP violation, Adelaide, Australia, 3-8 jul 1998*, edited by X. -H. Guo, M. Sevier, A. W. Thomas. World Scientific, 2000.
- [8] G. Isidori, hep-ph/9908399, *Presented at 1999 Chicago Conference on Kaon Physics (K 99)*, Chicago, 21-26 Jun 1999.
- [9] A. J. Buras, G. Colangelo, G. Isidori, A. Romanino, and L. Silvestrini, Nucl. Phys. **B566**, 3 (2000). Phys. Rev. **D63**, 014015 (2001).
- [10] K. P. Jungmann, hep-ex/9806003, in *Proceedings of Tropical Workshop on Particle Physics and Cosmology, San Juan, Puerto Rico, 1-7 Apr 1998*, edited by Jose F. Nieves. Amer. Inst. Phys., 2000.

- [11] G. Buchalla and A. J. Buras, Nucl. Phys. **B400**, 225 (1993); Nucl. Phys. **B412**, 106 (1994).
- [12] A. P. Heinson et al., Phys. Rev. **D51**, 985 (1995); T. Akagi et al., Phys. Rev. D 51 2061 (1995).
- [13] See e.g. P. H. Frampton, P. Q. Hung, and M. Sher, Physics Reports **330**, 263 (2000).

FIGURES

FIG. 1. Feynman graphs for the effective vertexes of the Z and γ for $\Delta S = 1$ processes $s \rightarrow d$. The self energy diagrams are omitted.

FIG. 2. Feynman graphs for the effective vertex of the g for $\Delta S = 1$ processes $s \rightarrow d$. The self energy diagrams are omitted.

FIG. 3. The function $C_0(x_F, b)$, appearing in the amplitude for the Z effective vertex is plotted in linear and logarithmic scale for $b = 0.001$ and $b = 0.0001$. The function $C_0(x_F)$, which is the first non vanishing coefficient in the Taylor expansion in b of $C_0(x_F, b)$ is also plotted.

FIG. 4. The logarithm of the function $D_0(x_F, b)$, appearing in the amplitude for the γ effective vertex is plotted versus the logarithm of x_F for $b = 0.001$ and $b = 0.0001$. The function $D_0(x_F)$, which is the first non vanishing coefficient in the Taylor expansion in b of $D_0(x_F, b)$ is also plotted.

FIG. 5. Box diagrams for $\Delta S = 1$ process $sd \rightarrow dd$. The corresponding box diagrams with the pseudo NG bosons $Re\tilde{\rho}'_i$ instead of the NG bosons $\tilde{\Omega}'_i$ are omitted.

FIG. 6. The function $B_0(x_F, b)$, appearing in the amplitude for the box diagrams in the process $sd \rightarrow dd$ is plotted in linear and logarithmic scale for $b = 0.001$ and $b = 0.0001$. The function $B_0(x_F)$, which is the first non vanishing coefficient in the Taylor expansion in b of $B_0(x_F, b)$ is also plotted.

FIG. 7. The function $B_{mix0}(x_F, x_M, b)$, appearing in the amplitude for the box diagrams in the process $sd \rightarrow dd$ is plotted in linear and logarithmic scale for $b = 0.001$ and $b = 0.0001$ versus x_M , with the condition $x_F = 10^{-4}x_M$.

FIG. 8. Feynman graphs for the $\Delta S = 1$ process $sd \rightarrow \mu e$. In the graph (e) the vertices are effective. The corresponding diagrams with the pseudo NG bosons $Re\tilde{\rho}'_i$ instead of the NG bosons $\tilde{\Omega}'_i$ are omitted.

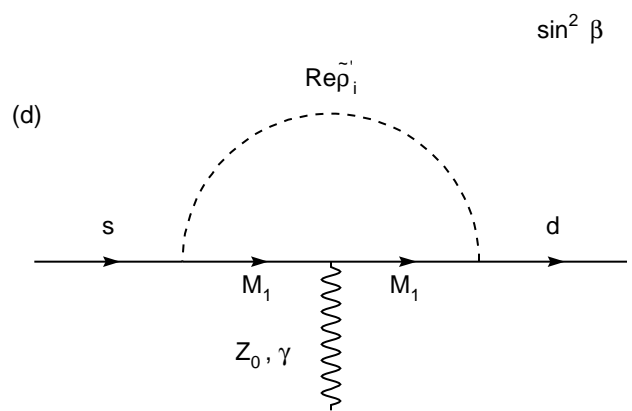
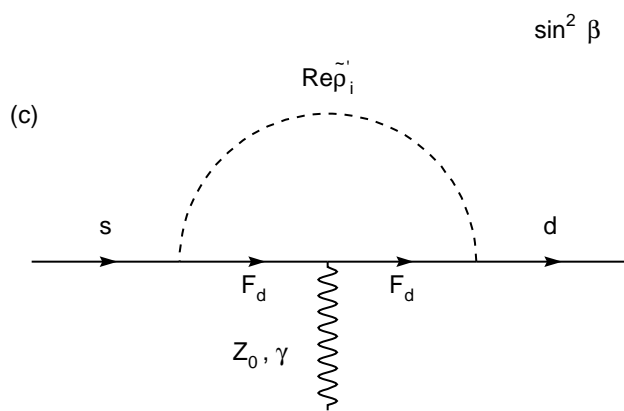
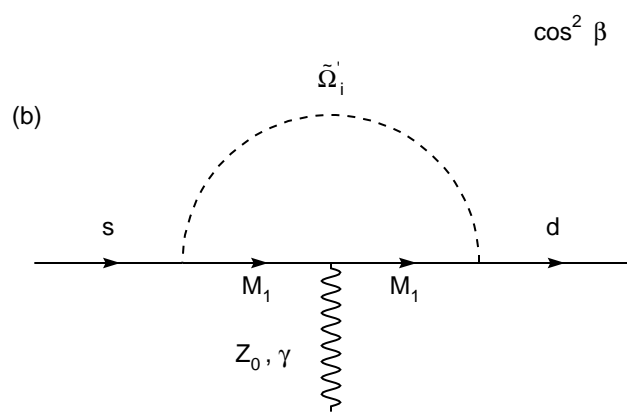
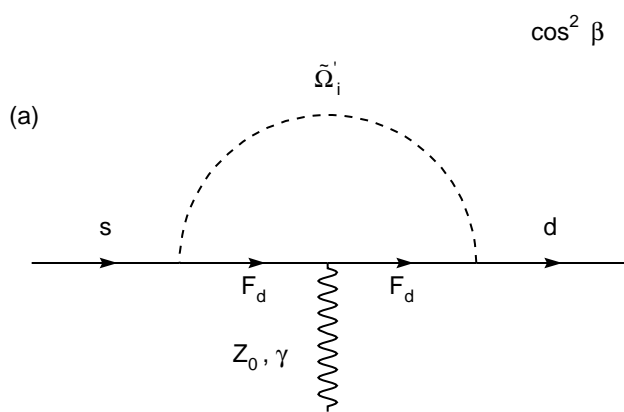
FIG. 9. The logarithm of the function $(C_{Lq} - C_{Rq})^2(C_{Ll}^2 + C_{Rl}^2)$, which appears in Eq. 76 for the $BR(K_L \rightarrow \mu e)$ is plotted versus $Log(x_M/x_F)$, for $b = 2.5 \cdot 10^{-4}$, $M_G = 200TeV$ and $x_F = 10^{-6}$.

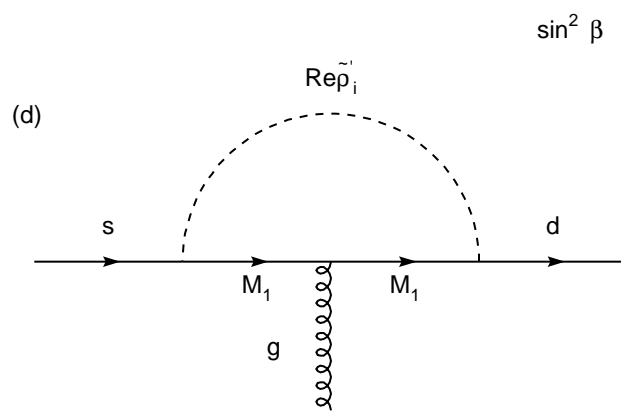
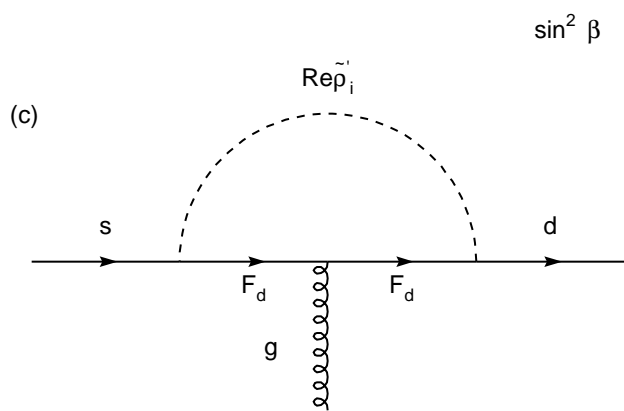
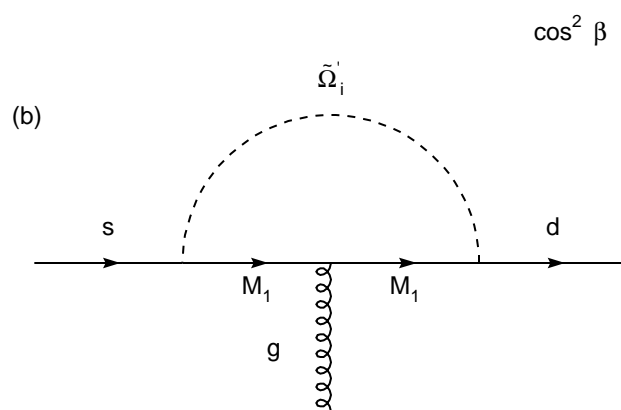
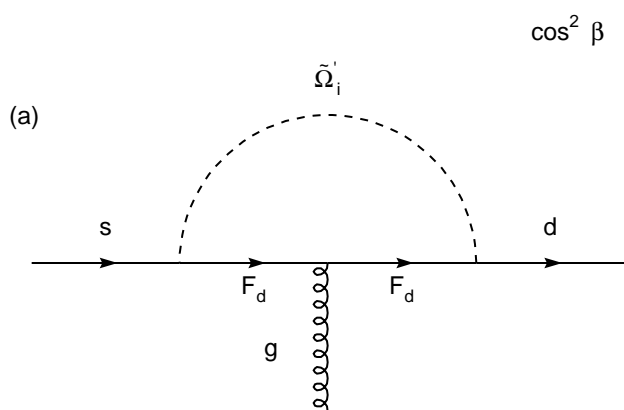
FIG. 10. The logarithm of $BR(K_L \rightarrow \mu e)$ is plotted versus $Log(x_M/x_F)$, for $b = 2.5 \cdot 10^{-4}$, $M_G = 200TeV$ and $x_F = 10^{-6}$. The lowest flat zone corresponds to $BR(K_L \rightarrow \mu e) = 6.65 \cdot 10^{-22}$, while the highest flat zone corresponds to $BR(K_L \rightarrow \mu e) = 1.02 \cdot 10^{-14}$.

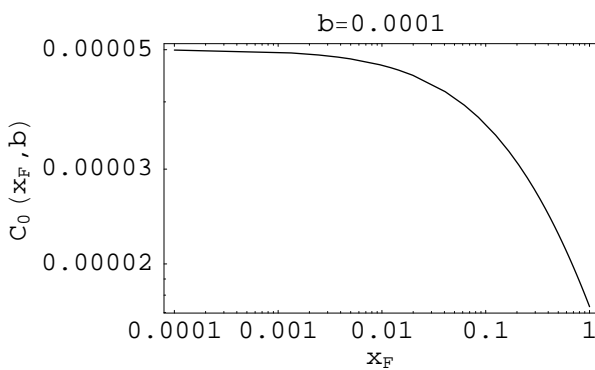
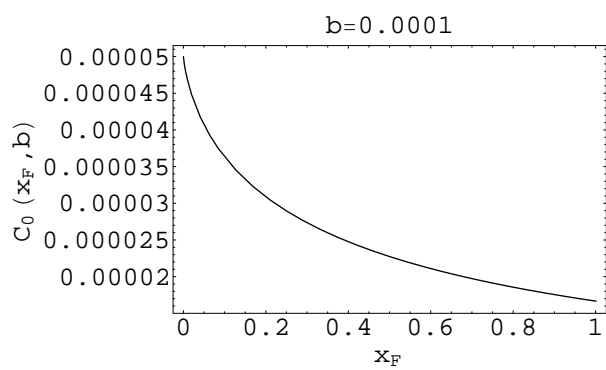
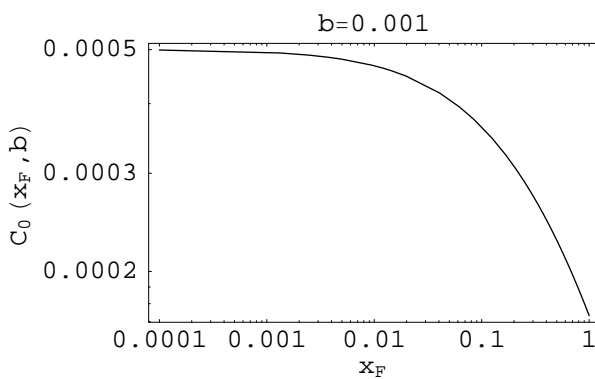
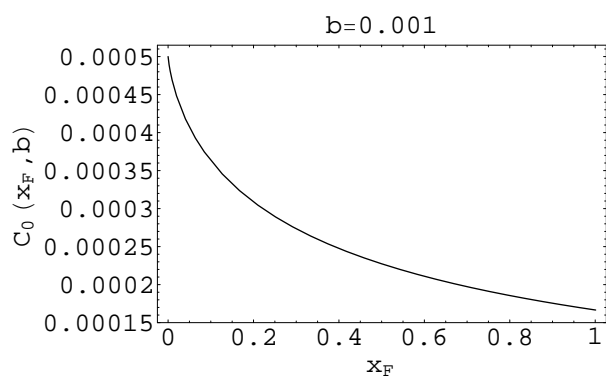
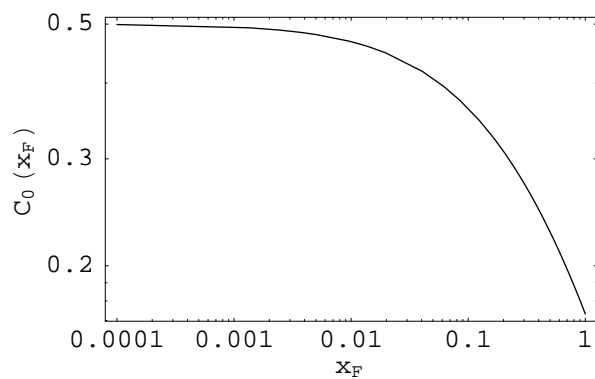
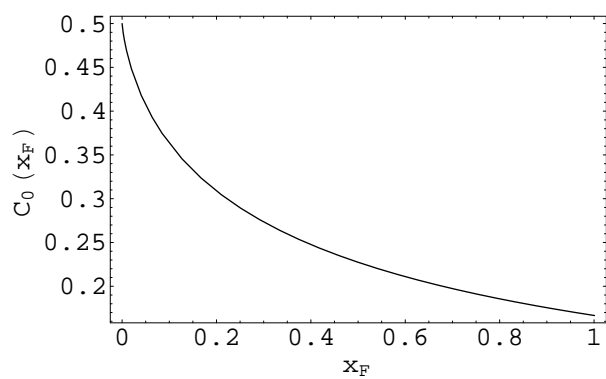
TABLES

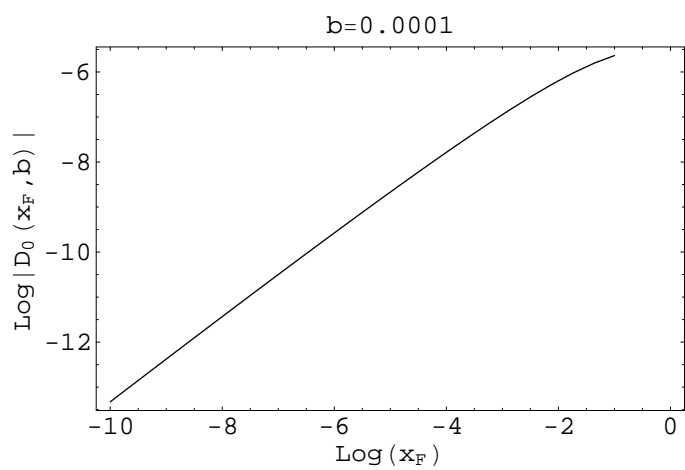
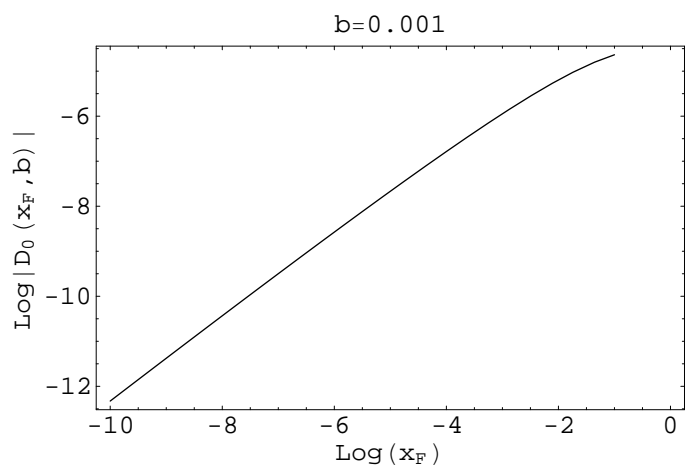
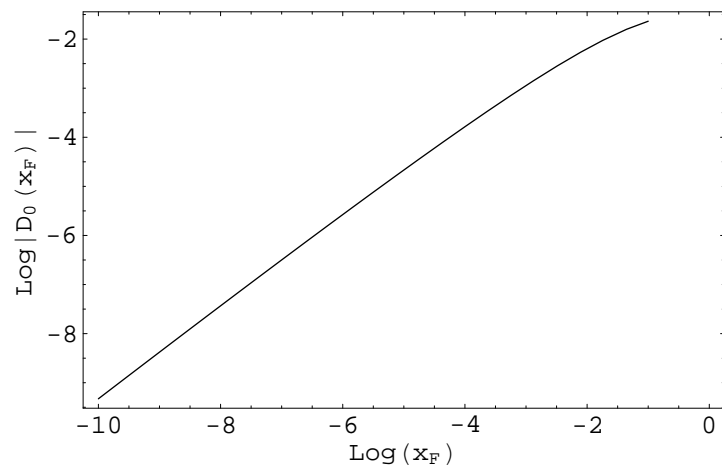
TABLE I. Particle content and quantum numbers of $SU(3)_c \otimes SU(2)_L \otimes U(1)_Y \otimes SO(N_f) \otimes SU(2)_{\nu_R}$

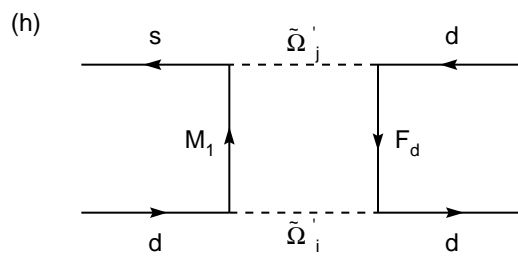
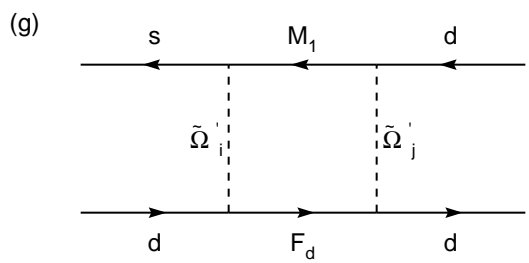
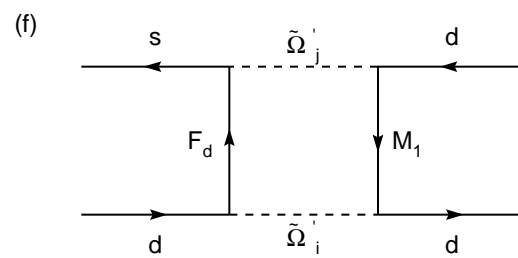
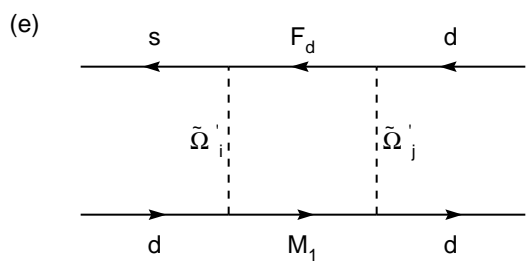
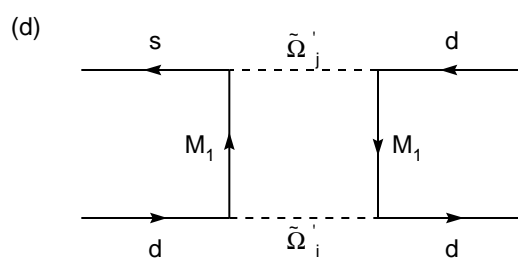
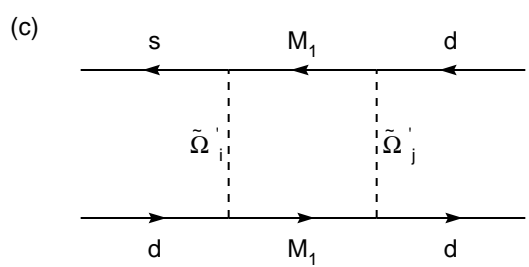
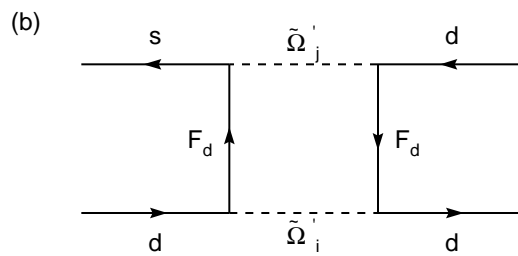
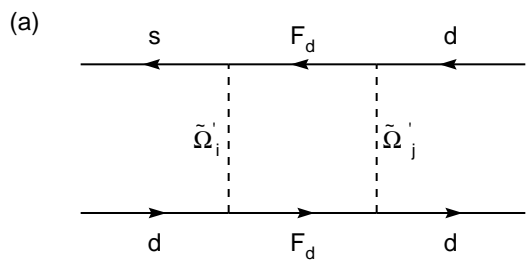
Standard Fermions	$q_L = (3, 2, 1/6, N_f, 1)$ $l_L = (1, 2, -1/2, N_f, 1)$ $u_R = (3, 1, 2/3, N_f, 1)$ $d_R = (3, 1, -1/3, N_f, 1)$ $e_R = (1, 1, -1, N_f, 1)$
Right-handed ν 's	Option 1: $\eta_R = (1, 1, 0, N_f, 2)$ Option 2: $\eta_R = (1, 1, 0, N_f, 2);$ $\eta'_R = (1, 1, 0, 1, 2)$
Vector-like Fermions for the lepton sector	$F_{L,R}^l = (1, 2, -1/2, 1, 1)$ $\mathcal{M}_{1L,R}^l = (1, 1, -1, 1, 1)$ $\mathcal{M}_{2L,R}^l = (1, 1, 0, 1, 1)$
Vector-like Fermions for the quark sector	$F_{L,R}^q = (3, 2, 1/6, 1, 1)$ $\mathcal{M}_{1L,R}^q = (3, 1, -1/3, 1, 1)$ $\mathcal{M}_{2L,R}^q = (3, 1, 2/3, 1, 1)$
Scalars	$\Omega^\alpha = (1, 1, 0, N_f, 1)$ $\rho_i^\alpha = (1, 1, 0, N_f, 2)$ $\phi = (1, 2, 1/2, 1, 1)$

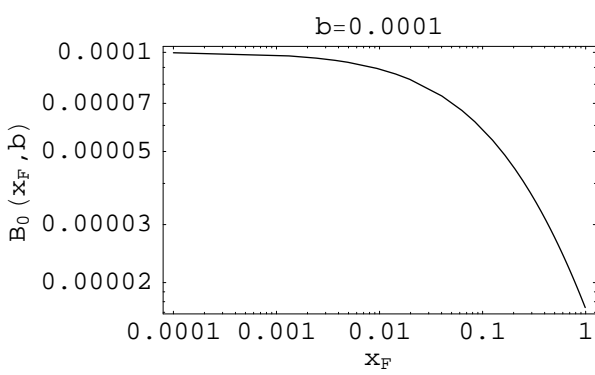
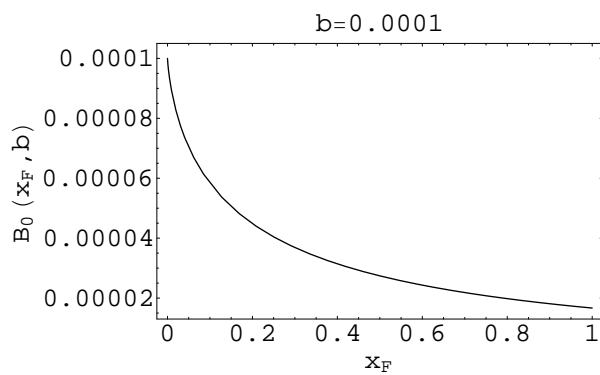
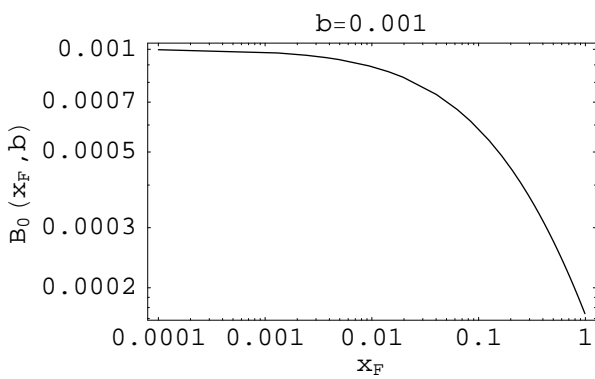
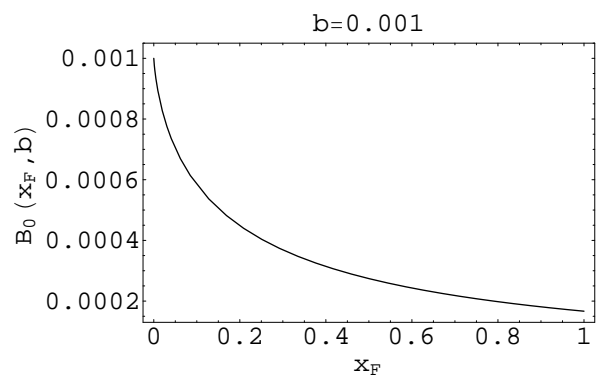
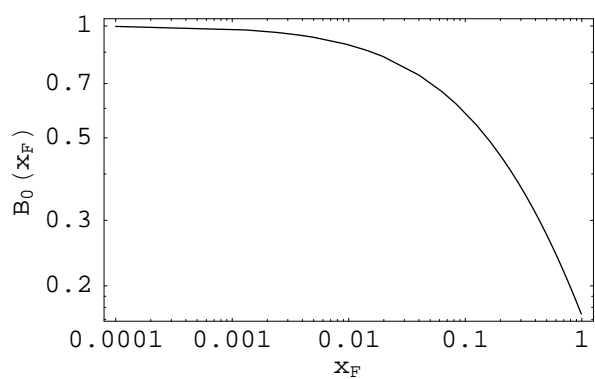
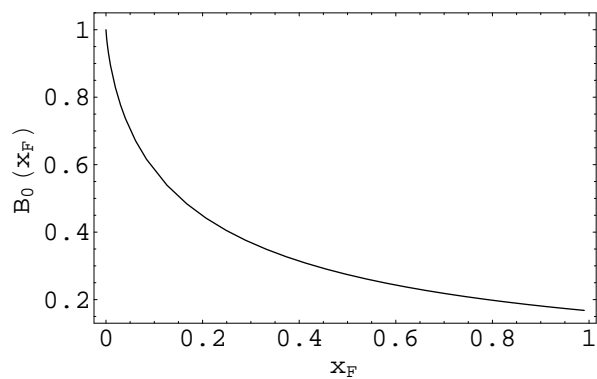


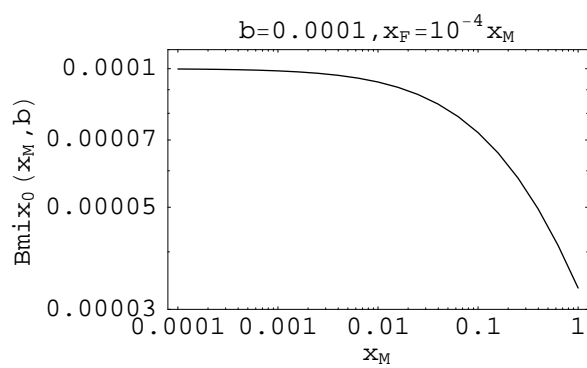
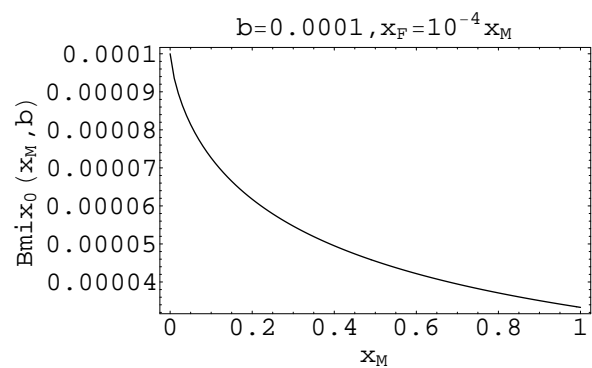
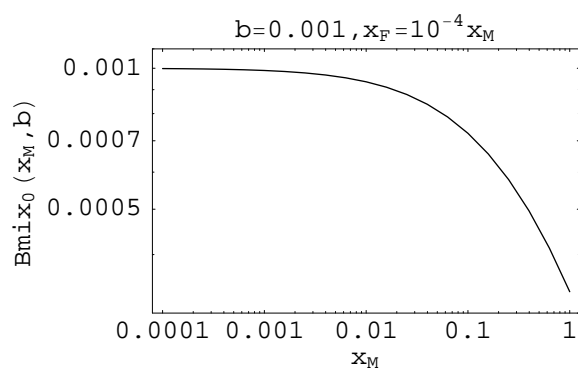
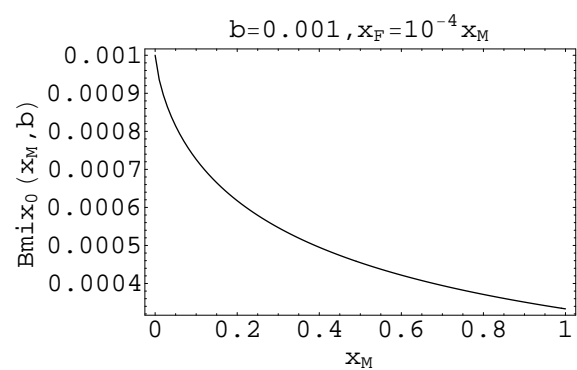




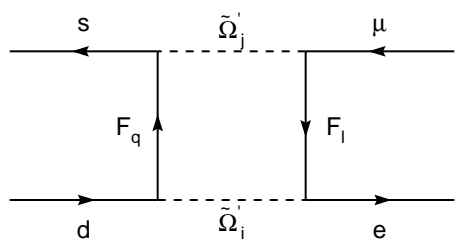




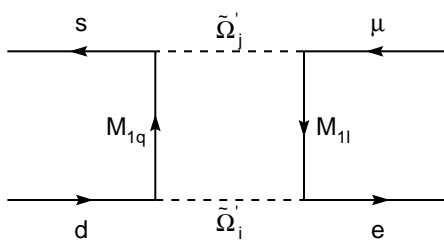




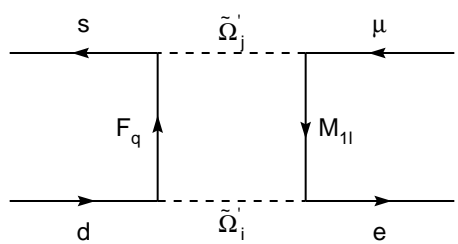
(a)



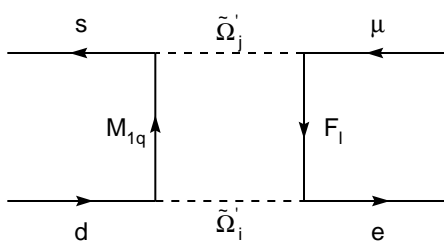
(b)



(c)



(d)



(e)

